Patterning of narrow porous SiOCH trenches using a TiN hard mask

Maxime Darnon, T. Chevolleau, D. Eon, R. Bouyssou, B. Pelissier, L. Vallier, O. R. Joubert, N. Posseme, T. David, F. Bailly, et al.

Patterning of narrow porous SiOCH trenches using a TiN hard mask

M. Darnon [a,*], T. Chevolleau [a], D. Eon [a], R. Bouyssou [a], B. Pelissier [a], L. Vallier [a], O. Joubert [a], N. Posseme [b], T. David [b], F. Bailly [c], J. Torres [c]

[a] LTM/CNRS, (CEA-LETI-Minatec), 17 rue des martyrs, 38054 Grenoble cedex 09, France
[b] CEA-LETI-Minatec, 17 rue des martyrs, 38054 Grenoble cedex 09, France
[c] STMicroelectronics, Central R&D, 850 rue J. Monnet, 38926 Crolles cedex, France

For the next technological generations of integrated circuits, the traditional challenges faced by etch plasmas (profile control, selectivity, critical dimensions, uniformity, defects, ...) become more and more difficult, intensified by the use of new materials, the limitations of lithography, and the recent introduction of new device structures and integration schemes. Particularly in the field of the interconnect fabrication, where dual-damascene patterning is performed by etching trenches and vias in porous low-k dielectrics, the main challenges are in controlling the profile of the etched structures, minimizing plasma-induced damage, and controlling the impact of various types of etch stops and hard mask materials. Metallic hard masks can help thanks to their high selectivity toward low-k materials, and by avoiding low-k exposure to potentially degrading ashing plasmas. In this paper, we will present some key issues related to the patterning of narrow porous SiOCH trenches with a metallic (TiN) hard mask. Narrow trenches (down to 40 nm width) can be opened into TiN with a critical dimensions bias (around 10 nm) attributed to carbon and silicon containing deposits on the photoresist and TiN sidewalls during the etching. Porous SiOCH etching using a TiN hard mask instead of the conventional SiO_2 hard mask may lead to severe profile distortions, attributed to TiF_x compounds which settle on the trenches sidewalls. A chuck temperature of 60 °C and fluorine-rich plasmas are required to minimize those distortions. An etching process leading to almost straight porous SiOCH profiles presenting a slight bow has been developed. However a wiggling phenomenon has been evidenced for the etching of narrow and deep trenches. This phenomenon is attributed to the highly compressive residual stress in the TiN hard mask, which is released when the dielectric is not mechanically strong enough to withstand it.

1. Introduction

In CMOS technologies, the race towards lower dimensions and better performances leads to the use of copper/ultra low-k interconnects. The ITRS predicts an interconnect pitch of 90 nm with an effective dielectric permittivity between 2.5 and 2.8 for the first level of metal for the 45 nm node targeted in 2008. Such an effective dielectric constant can be achieved with the integration of a porous dielectric material. Some difficult challenges need to be overcome with the porous dielectric materials. Etching, ashing and cleaning processes of these porous materials in narrow structures are very challenging because they change the material properties, which impacts the electrical and reliability performances [1]. For the integration of porous SiOCH in dual damascene architectures, a dual hard mask strategy has been developed to prevent a direct exposure of the dielectric material to ashing plasmas [2]. Among the different integration schemes, it is already anticipated that conventional inorganic hard masks (such as SiO_2 and SiC) cannot be implemented in the next IC generations because of their poor etching resistance to fluorocarbon-based plasmas which leads to a low selectivity and a significant faceting [3]. New hard masks such as metallic and organic materials are currently investigated as potential candidates to replace the conventional SiO_2 and SiC inorganic hard masks. Metallic and organic materials (TiN, TaN, carbon-rich layers,...) have a different chemical nature than dielectric materials and therefore exhibit better hard mask capabilities than conventional hard masks [4].

This study is devoted to the etching of narrow porous SiOCH trenches using a TiN hard mask. The experimental work consists in studying the etch profiles of narrow porous SiOCH trenches as a function of the etch chemistry and plasma conditions. The main goals are to determine the most important critical dimension issues (profile distortion, hard mask faceting, ...) and to control the profile of narrow porous SiOCH trenches.

* Corresponding author.
E-mail address: mdarnon@gmail.com (M. Darnon).

2. Experimental setup

200 mm silicon wafers have been used during this study. They were coated with two different low-k materials: (1) a porous SiOCH (300 nm thick deposited by spin coating) and (2) a dense SiOCH (800 nm thick deposited by PECVD). The porous SiOCH exhibits a dielectric constant of 2.3 with a porosity of about 45%. The dielectric constant of the dense SiOCH is 2.9. Rigorously speaking, the dense material also exhibits some micro porosity, estimated to be about 8% [5]. However, the SiOCH deposited by PECVD will be considered as a dense SiOCH material in this work. More details on these materials can be found in previous papers [6,7] and in Table 1.

The patterning of SiOCH trenches has been performed with a dual hard mask strategy using a metallic hard mask. The stack investigated is the following: a SiO_2 (TEOS) capping layer of 40 nm which is coated on the low-k material before the deposition of 45 nm thick TiN (PVD deposition). The wafers are patterned either with an electron beam lithography to get aggressive trench dimensions down to 50 nm width or with a specific 248 nm lithography for chemical topography analyses [8].

Etching experiments are performed in a Tokyo Electron Limited DRM™ chamber for the etching of the dielectrics layers (SiO_2 and SiOCH) and in an Applied Materials DPS™ chamber for the etching of the TiN hard mask. The schematics of the DRM™ and DPS™ reactors have been previously described elsewhere [9,10]. The etching platform, on which the DPS™ chamber is mounted, is connected to an X-ray photoelectron spectroscopy (XPS) surface analysis system (customized 220I system from VG scientific) via a transfer chamber.

The TiN hard mask opening is carried out in the DPS™ plasma etcher at a cathode temperature of 50 °C. Before each process, a cleaning process (a Cl_2 plasma followed by a SF_6 / O_2 plasma) and a conditioning process are performed on a blanket silicon wafer in order to get reproducible etching conditions from wafer to wafer [11]. After TiN opening, the remaining photoresist is removed in an oxygen-based plasma. Then the etching of the dielectric layers (SiO_2 and low-k material) is done in the DRM™ plasma etcher. A cleaning (O_2 plasma) and a conditioning process on a blanket silicon wafer are also performed prior to each dielectric etch process.

After etching in the DPS™ plasma reactor, wafers can be transferred under vacuum into the XPS analysis chamber, where the surface composition of the etched material can be analysed quasi in situ. Chemical topography analyses by XPS are performed to determine the surface composition of the trench sidewalls. The XPS apparatus uses a non monochromatized X-ray source consisting of a water-cooled standard twin-anode, or a monochromatized X-ray source. A constant dwelling time of 100 ms and pass energy of 20 eV are chosen. The surface analysed is about 1 mm in diameter. The chemical concentration of the elements present at the surface of the material is extracted from their core level energy regions. Peaks areas are determined after a spectral deconvolution based on an iterative numerical fitting procedure. Individual line shapes are simulated with the combination of Lorentzian and Gaussian functions. A Shirley function is used to perform background subtraction. Each element concentration is obtained by dividing the peak area by the corresponding Scofield cross section (F1s: 4.43, Si2p: 0.87, O1s: 2.93, Ti2p: 7.91, N1s: 1.8, C1s: 1) [12]. The total concentration of all elements detected on the surface is equal to 100%. Absolute quantitative concentrations have to be taken with great care, since with metallic layers, and in particular Ti, ill-defined satellites can be included in the metallic element background [4,13–15]. However, using exactly the same fitting procedure for the Ti*2p* line shape, the evolution of the concentration of each element can be considered as the relative evolution of the composition of the analysed surface as a function of the etch chemistry [4].

The principle of the chemical-topography analysis technique using XPS is described in greater details elsewhere [8,16]. A reticule for optical lithography has been especially designed to perform chemical topography analysis. Each die consists of different zones: regular arrays of trenches, patterned mask zones and unpatterned zones. The area of each zone is at least 9 mm^2. By moving the wafer in the *x*, *y* and *z* directions in the XPS analysis chamber, the X-ray beam can then be focused on one individual zone, the resulting signal being the average signal of many identical dielectric trenches and lines in the case of a zone of regular arrays. When we analyse an array zone in the perpendicular mode (i.e. the detector axis is perpendicular with the trenches direction), this average signal originates from the top of the dielectric and part of the trenches sidewall (Fig. 1). The dimensions of the trenches and the spaces between trenches are different from zone to zone. As we only want to study the sidewalls of the trenches (and not the bottom), we have to choose an array which enables us to select the desired portion of the trenches sidewalls only [8,16]. Fig. 1 shows that with a 45° electron analyser, the portion of the trenches sidewalls analysed equals the width of the trench. Since in our conditions the trench depth is around 335 nm after the etching process (250 nm of ULK + 40 nm of SiO_2 + 45 nm of TiN), the trench width must not exceed this value if we want to analyse the trench sidewalls only. Two different arrays zones are well adapted for our experiments. In the first array, the dielectric line width is 300 nm and trench width is 300 nm. In the second array, the dielectric line width is 300 nm and the trench width is 200 nm.

To characterize the surface composition of the trench sidewalls, we have developed an experimental procedure derived from the chemical-topography analyses described by Pargon et al [16]. In our experimental conditions, the hard mask is a floating conductor on an insulating material. Therefore, we cannot electrically separate the contributions originating from the hard mask from those originating from the trenches sidewalls. To succeed in separating the contributions coming from the hard mask and those coming from the trenches sidewalls, two acquisitions are made on two different zones present on the wafer. The first acquisition is performed on a blanket hard mask zone. The second acquisition is performed in the perpendicular mode on one of the specific array zones to get information on the chemical composition of the trenches sidewalls (see Fig. 1). This analysis gives access to an average surface composition, combining the signal originating from both the top of the hard mask and a part of the trench sidewalls.

Table 1
Parameters used to estimate the flow of fluorine consumption during porous SiOCH, dense SiOCH and Si etching with the baseline process

Parameter	Unit	Common	Porous SiOCH	Dense SiOCH	Si
Density	$g.cm^{-3}$		0.9	1.3	2.33
Etched depth	cm		2.3×10^{-5}	3×10^{-5}	2×10^{-5}
Etching time	s		60	90	30
%Si	%		24	16	100
%O	%		11	22	0
%C	%		30	14	0
%H	%		34	48	0
Surface	cm^2	314			
Volume	cm^3	42000			
Open ratio	/	0.8			
$\mathbf{m_{Si}}$	amu	28			
$\mathbf{m_O}$	amu	16			
$\mathbf{m_C}$	amu	12			
$\mathbf{m_H}$	amu	1			
Scavenging rate of fluorine	$\mathbf{cm^{-3}.s^{-1}}$		$\mathbf{1.1 \times 10^{14}}$	$\mathbf{1.5 \times 10^{14}}$	$\mathbf{6 \times 10^{14}}$
Estimated fluorine flow	**sccm**		**10**	**14**	**56**

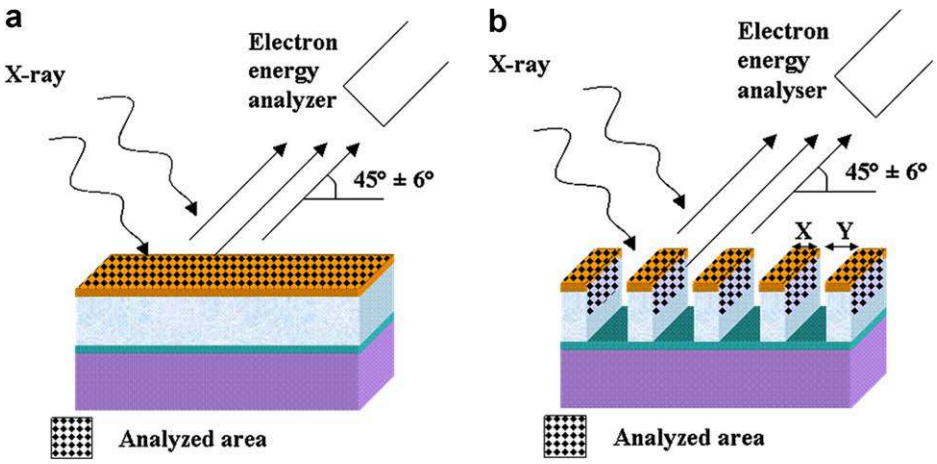

Fig. 1. Schematic of the experimental procedure used to analyse the trenches sidewall modification after etching (a) acquisition on mask area, (b) acquisition on trenches arrays in perpendicular mode.

If we call X the width of the line, and Y the width of the trench, the signal of one atomic element coming from the hard mask and the sidewall of the trenches represents $X/(X+Y)$ and $Y/(X+Y)$ of the total signal coming from the patterned zone, respectively [16].

Knowing the contribution originating from the hard mask and the X and Y parameters (measured by SEM cross-section), we can extract the contributions originating from the trenches sidewalls only. For each element, we have:

$$[A]_{\text{sidewalls}} = \frac{X+Y}{Y}\left[[A]_{\text{arrays}} - \frac{X}{X+Y}[A]_{\text{HM}}\right],$$

where $[A]_{\text{sidewalls}}$, $[A]_{\text{arrays}}$ and $[A]_{\text{HM}}$ represent the contribution of the element on the sidewalls, on the arrays zone, and on the hard mask blanket zone, respectively. In our case, we make the assumption that the surface composition of the TiN recorded on a blanket zone is very similar to this of the TiN on an array zone. This hypothesis is supported by the fact that the top of the hard mask and the blanket area are identically exposed to the plasma. We also consider that the hard mask thickness is negligible compared to the trenches height (less than 15%) and that the surface composition is similar on both SiO_2 capping and low-k sidewalls. Furthermore, the quantitative surface analysis is depending on several aspects such as the relative response of the analyser across the acceptance cone and the angular response of the electron analyser. However, in our conditions, these effects can be considered negligible compared to errors due to the extraction method. This method is then not very accurate in absolute value, but is satisfactory enough to give trends on the evolution of the trench sidewalls surface composition as a function of the etching parameters.

3. Experimental results and discussion

3.1. TiN Hard mask etch process

We have first developed a specific etching process to transfer the resist patterns into the TiN hard mask. The process is composed of two steps: a breakthrough (BT) to remove the TiO_2 overlayer and a main etch (ME) which is highly selective with respect to the underneath SiO_2 capping layer. The BT is an Ar-based plasma while the main etch is a Cl_2-based plasma. A real-time etch process control is achieved by monitoring the optical emission of Ti at 365 and 400 nm to determine the endpoint when landing on the SiO_2 capping layer (as shown in Fig. 2). The BT step has been optimized to completely remove the TiO_2 overlayer before starting the ME. The TiO_2 removal efficiency has been investigated on blanket TiN wafers for different BT conditions (etching chemistry and plasma parameters). Before the breakthrough, the top surface of TiN is mainly composed of Ti (30%), O (53%) and N (9%) indicating the presence of a TiO_x layer (see Table 2). After BT with a pure Ar plasma, XPS analyses show that TiO_2 is hardly removed since the surface is composed of Ti (34%), O (45%) and N (14%). When Cl_2 is added in the Ar plasma, a thin mixed TiO_2 / $TiCl_x$ layer is present on the top surface of TiN (33% of Ti, 44% of N, 6% of O and 14% of Cl). This result indicates that Cl_2 addition leads to the quasi removal of the TiO_2 overlayer. Fig. 3 shows the SEM pictures of the TiN etching profiles obtained on patterned wafers with a) a BT using a pure Argon plasma and b) a BT with Cl_2 addition. In the case of an almost complete TiO_2 removal (BT with Cl_2 addition), a good hard mask opening step is achieved with straight etch profiles in TiN and without visible residues on the SiO_2 surface underneath. Oppositely, when TiO_2 is hardly removed during the BT (using a pure Ar plasma), a lateral consumption in TiN is observed with an important amount of Ti residues on the SiO_2 underneath. Those residues are attributed to the presence of TiO_x residues before the ME which lead to micromasking during the ME. The lateral consumption in TiN can be explained by non uniform etching of the trenches due to microtrenching which is induced by the titanium oxide overlayer. Indeed the sputtering yield of titanium oxide is

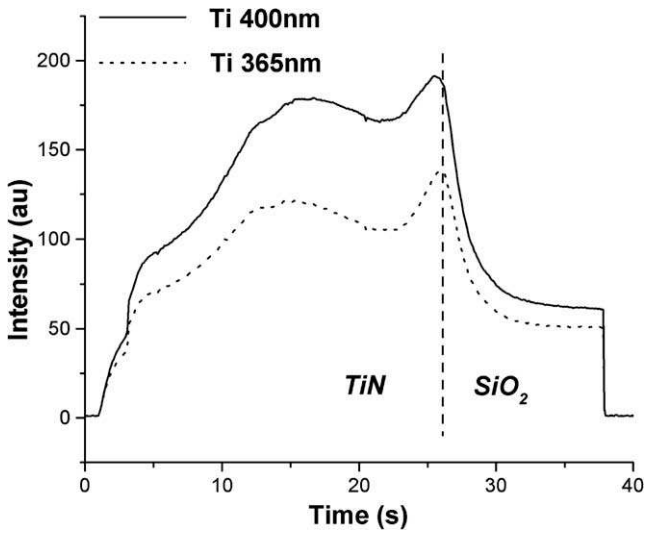

Fig. 2. Endpoint detection of TiN etch process by optical emission spectroscopy.

Table 2
Chemical composition of the top surface of TiN determined by XPS: as deposited, after breakthrough (BT) without chlorine (4 mTorr/100 sccm Ar/1000 W of source power and 100 W of bias power), and after breakthrough with chlorine (4 mTorr/100 sccm Ar/20 sccm Cl_2/1000 W of source power and 100 W of bias power)

	F1s (%)	O1s (%)	Ti2p (%)	N1s (%)	C1s (%)	Cl2p (%)
TiN as deposited	2	53	30	9	7	–
BT wo Cl_2	3	45	34	14	3	–
BT w Cl_2	–	6	33	44	3	14

higher at the edges of the trench than at the center due to 1) ion reflection from resist sidewalls to the bottom and/or 2) ion deflection from localized charging of the insulating resist [17]. Thus, the etching process removes the titanium oxide layer faster at the edges than at the center and consequently TiN is over exposed to the reactive chlorine plasma at the corner. The over exposition of TiN sidewalls can result in a lateral etching. In addition, the presence of TiO_x at the center induces a lower loading of reactive chlorine species during the etching process since the reactivity of TiO_x layer to chlorine plasma is low. This can lead to higher reactive chlorine species concentration available at the corner which can amplify the lateral consumption. These results show that the BT has a strong impact on the TiN etch profile and that the best results are obtained by adding Cl_2 in the BT chemistry (Cl_2/Ar gas mixture). The ME is an etch process using a Cl_2/Ar gas mixture with less ionic bombardment than the BT in order to be selective with respect to the SiO_2 capping layer underneath. An optimization of the ME shows that the Cl_2/Ar ratio, source and bias power control the TiN etch rate. The source and bias power also have an impact on the residue formation on the SiO_2 surface underneath. It has been shown that higher source and bias powers lead to higher etch rates and a lower amount of residues [18].

Critical dimension (CD) measurements show a deviation between the initial trench CD and the trench CD after TiN etching (so called CD_{bias}). A CD_{bias} of about 10 nm is measured indicating a decrease in CD (lower trench width). A change in CD is widely observed after plasma etching, and is attributed to the formation of passivation layers on the sidewalls of the structures [8,19–21]. In our case, the decrease in CD can be explained by the formation of passivation layers on the photoresist and TiN sidewalls during the etching of TiN. We have performed chemical topography analysis by XPS in order to determine the passivation layers on the photoresist sidewalls. A first XPS analysis has been performed after partial etching of TiN, and a second one after complete etching of TiN with an overetch time of 20%. Since the photoresist thickness (400 nm) is higher than the trench width (200 or 300 nm), the XPS analyses provide only information on the passivation layer formed on the photoresist sidewalls. Fig. 4 shows that the surface of the sidewalls is made of 59% of C, 28% of Cl, 8% of O, 4% of N. Based on core level spectra analyses, oxygen, nitrogen and part of the carbon come from the photoresist itself while chlorine and the remaining carbon originate from $C_xH_yCl_z$ resist-etch by-products. Indeed it has been shown [16,22] that in Cl_2-based chemistries $C_xH_yCl_z$ species are formed by the chemical sputtering of the chlorine-rich resist surfaces. Such non-volatile $C_xH_yCl_z$ etch by-products sputtered in the gas phase get redeposited on the resist sidewalls leading to the formation of a passivation layer. After complete etching of TiN with an overetch time of 20%, the surface composition of the sidewalls is different and composed of 15% of C, 44% of Cl, 22% of Si and 19% of O (Fig. 4). These results indicate that $C_xH_yCl_z$ resist etch by-products are still present, but SiO_xCl_y compounds are also detected on the trench sidewalls. SiO_xCl_y passivation layers are known to be formed on poly-silicon gate sidewalls when silicon is etched using chlorine/oxygen based chemistries [8,19–21,23]. It is now well known that halogen-silicon ($SiCl_x$) etch by-products presenting a low volatility get redeposited on the feature sidewalls where they are subsequently oxidized by the oxygen radical present in the gas mixture leading to the formation of a SiO_xCl_y passivation layer [19,20]. In our case, the slight etching of the underneath SiO_2 during the over etch time generates enough $SiCl_x$ species and oxygen radical into the plasma explaining the presence of SiO_xCl_y compounds on the photoresist sidewalls.

The decrease of the trench CD during the etching of TiN can therefore be attributed to the deposition of a CHCl–SiOCl mixed passivation layer on the photoresist sidewalls and probably also on the TiN sidewalls. During the etching of TiN in a Cl_2-based chemistry, $C_xH_yCl_z$ species come from the sputtering of the chlorine rich resist surface while SiO_xCl_y compounds originate from the etching of the SiO_2 underneath.

3.2. Dielectric etch process

3.2.1. Effect of metallic hard mask on the dielectric etch process

Using metallic hard masks can drastically impact the characteristics of typical dielectric etching processes. We have investigated the influence of TiN hard mask on a standard etching process by comparing the trench profiles of porous SiOCH masked with a conventional SiO_2 mask and with a TiN hard mask [3]. The cross

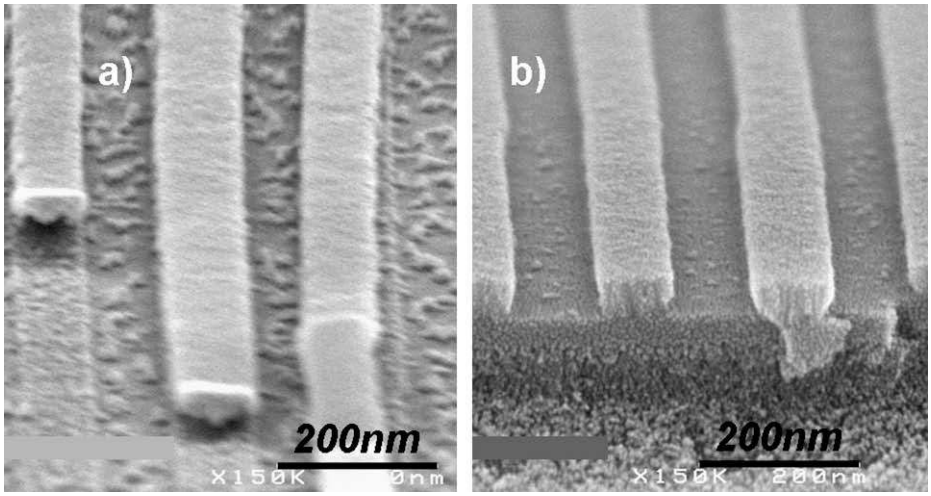

Fig. 3. SEM pictures after hard mask opening (BT + ME + stripping) with different BT: (a) pure Ar plasma, (b) with Cl_2 addition in the Ar plasma.

section SEM pictures (Fig. 5) indicate that straight profiles are observed in SiO_2 masked trenches while TiN masked trenches exhibit severe profile distortions. The profile distortions obtained with the TiN hard mask are explained by the presence of non uniform deposits on the trench sidewalls. This result clearly indicates that the metallic hard mask has a strong impact on the etching of porous SiOCH dielectric features in fluorocarbon-based plasmas.

It is well known that during the etching of SiOCH-based dielectric masked with photoresist or inorganic masks (SiO_2, SiC) a thin and conformal fluorocarbon layer (few nanometers) settles on the sidewalls of the dielectric trenches [24,25]. This fluorocarbon layer originates from fluorocarbon radicals present in the plasma which get deposited on the dielectric sidewalls. When the dielectric is patterned using a TiN hard mask, a non conformal deposit is formed on the dielectric patterns. The deposit is preferentially localized at the top of the patterns (Fig. 5). During the etching process, the deposit is slowly formed as the etching proceeds and tends to block the etching of the dielectric, leading therefore to a strong profile distortion (Fig. 5). When plasma conditions leading to heavy deposition are used, the trench can be entirely blocked by the deposit which prevents the complete etching of the trench.

The chemical analysis of the deposit is difficult since chemical topography analysis can not be performed on highly distorted patterns. Thus a specific experiment (Fig. 6) has been conducted in order to be able to analyse the chemical nature of the deposits formed on the patterns sidewalls. We have analysed the deposits formed on the sidewalls of pre-patterned structures patched on a standard wafer during the etching process. The pre-patterned structures are defined as follows: SiO_2 trenches have been etched using a conventional SiC hard mask with the XPS reticule. After all the etching steps (etching of SiC and SiO_2), an oxygen-based plasma has been performed to remove the remaining photoresist and the fluorocarbon passivation layer on the SiO_2 trench sidewalls. SEM cross section shows that SiO_2 trenches are obtained with straight profiles and free of fluorocarbon passivation layer (Fig. 7). A coupon of this wafer with a size corresponding to several dies is fixed on a standard patterned wafer used in this work after the etching of TiN and ashing of the remaining photoresist. The standard wafer with the coupon is etched with the typical fluorocarbon etching process used for SiOCH trenches masked with SiO_2. SEM cross section pictures of the coupon show (Fig. 7) that a huge amount of deposits is formed on the sidewalls of SiO_2 trenches. In such a configuration, chemical topography analyses by XPS are reliable since the SiO_2 trench profiles are hardly distorted after the etching process. Chemical topography analyses by XPS show that the surface of the trench sidewalls is composed of 24% of silicon and 25% of oxygen and also 11% of titanium and 39% of fluorine and less than 1% of carbon. The Ti*2p* core level spectrum (Fig. 8) presents only two peaks at 461 and 466.8 eV which are both attributed to TiF_x bonds (Ti*2p3/2* and Ti*2p1/2* doublet, respectively) [4]. The silicon and oxygen observed on the sidewalls are supposed to originate from SiO_2 or eventually from a SiOF modified surface. The XPS analyses indicate that the deposits are mainly TiF_x metallic etch by-products. In order to confirm these results, we have performed another simple experiment: a coupon coated with a photoresist film is fixed on a standard patterned wafer used in this work (after TiN etching and ashing of the remaining photoresist). As previously, the wafer with the coupon are etched with the standard etching process used for SiOCH trenches masked with SiO_2. XPS analyses show the photoresist top surface is covered by TiF_x compounds with a very small amount of oxygen and silicon (less than 3%). Top view SEM pictures (not shown here) indicate the presence of deposits on the photoresist surface which is well correlated with the presence of TiF_x species.

Those experiments point out that the deposits observed on the dielectric sidewalls after the etching process are TiF_x compounds. Such TiF_x species originate from the etching or sputtering of the fluorine rich TiN surface during the fluorocarbon-based plasma and get redeposited on the trench sidewalls.

3.2.2. Impact of plasma parameters on profile control

We have developed a baseline process in the TEL DRM™ plasma etcher for the etching of p-SiOCH trenches masked with a TiN hard mask. The plasma conditions are: 87 sccm of CF_4, 250 sccm of

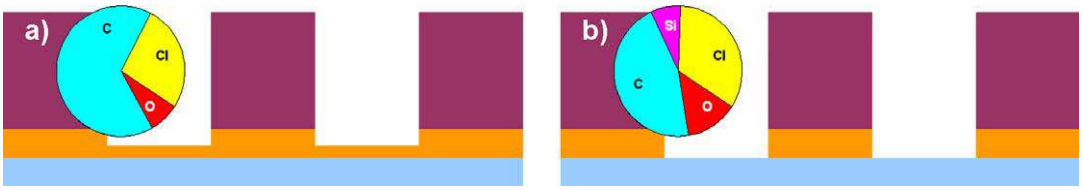

Fig. 4. Chemical composition of photoresist sidewalls determined by XPS after (a) partial TiN opening, (b) complete TiN opening with 20% over etch.

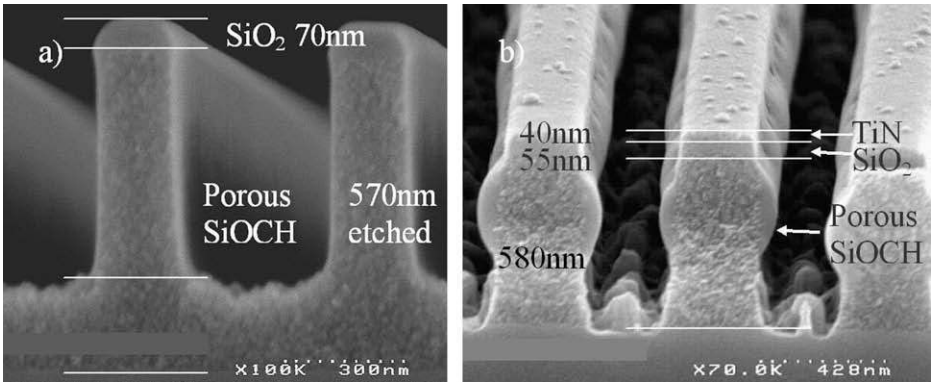

Fig. 5. Porous SiOCH trenches etched with (a) a SiO_2 hard mask, (b) a TiN hard mask.

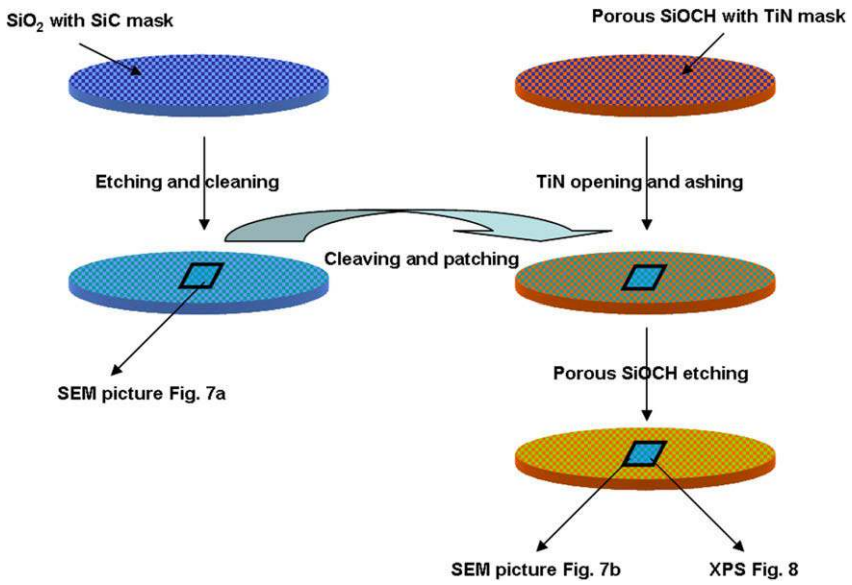

Fig. 6. Schematic of the coupon experiment used to determine the chemical nature of the deposits formed on trenches sidewalls.

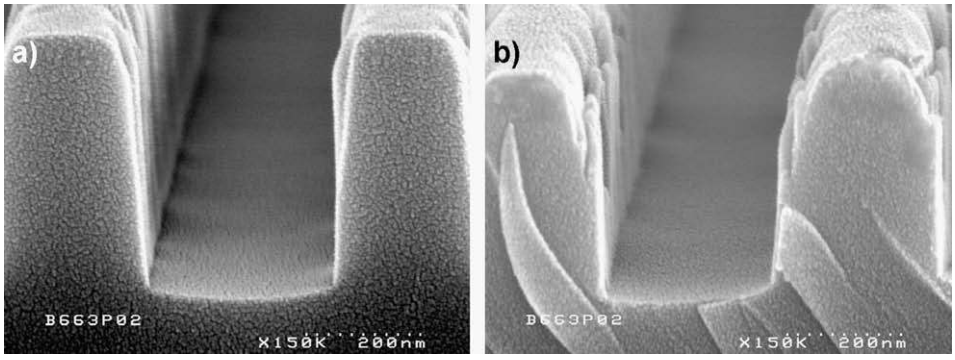

Fig. 7. SEM picture of SiO_2 trenches patched on a TiN / SiO_2 wafer (a) before etching, (b) after etching.

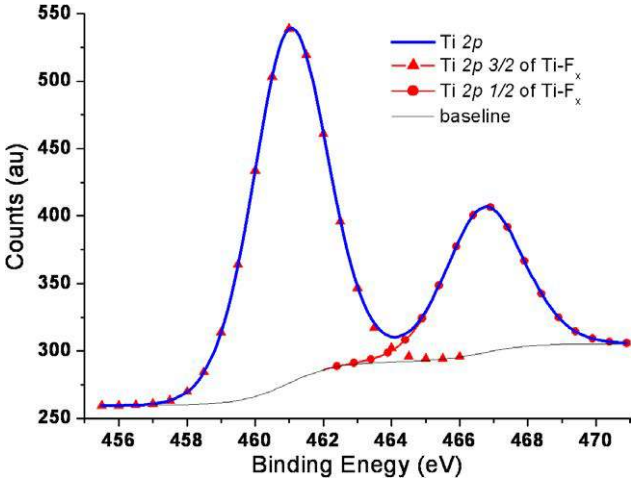

Fig. 8. XPS spectra of Ti*2p* core level on the trenches arrays.

Argon, 120 mTorr and 400 W of source power. Contrary to the process used in previous experiments, the substrate temperature is fixed at 60 °C instead of 20 °C. In those conditions, straight trench profiles are obtained with a slight bow and no deposits are observed on the trench sidewalls (Fig. 9). Chemical topography analyses by XPS show that the surface of the sidewalls is composed of 15% of silicon, 19% of oxygen, 17% of carbon, 49% of F and 1% of Ti. This composition indicates a fluorine rich surface and the presence of a fluorocarbon passivation layer on the trench sidewalls. The low amount of Ti (within the experimental precision) confirms that no TiN-based etch by-product are significantly deposited on the trench sidewalls during the etching.

We have evaluated the impact of the chuck temperature on the trench profile as shown in Fig. 9. Trench profile distortions are observed (Fig. 10) at lower wafer temperature (20 °C). This strong profile distortion is attributed to the redeposition of TiN etch by-products on the trench sidewalls. Chemical topography analyses by XPS have been performed on the patterned structures at 20 °C in order to determine the surface composition of the sidewalls (Fig. 10). A fluorocarbon passivation layer is observed with a significant amount of Ti (10%) which confirms that the deposits originate from TiN etch by-product redeposition. On the other hand, no significant amount of Ti was detected on the trench sidewalls with a substrate temperature of 60°. These results show that the presence of Ti can be strongly minimized by increasing the wafer temperature.

We have also evaluated the impact of the plasma parameters (etching chemistry, pressure, source power) and material properties

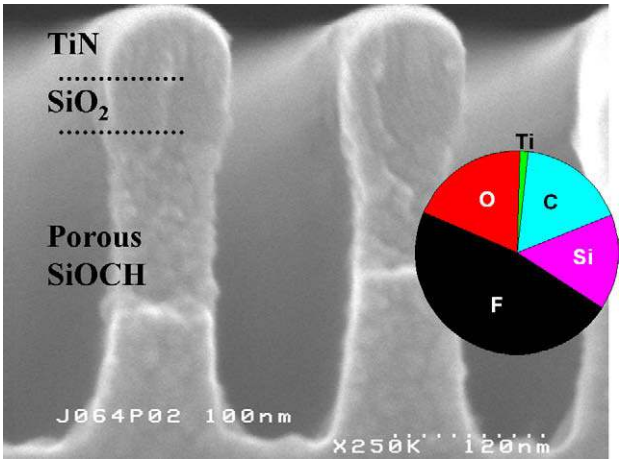

Fig. 9. Porous SiOCH trenches etched with the baseline process and chemical composition of the sidewalls determined by XPS.

on the trench profiles (Fig. 11) starting from the baseline process (87 sccm of CF_4, 250 sccm of Argon,120 mTorr and 400 W of source power and 60 °C). Lowering the pressure leads to a strong profile distortions due to an important redeposition of TiN etch by-products on the trench sidewalls. With the addition of a polymerizing gas such as CH_2F_2, a slight profile distortion is also evidenced which is also attributed to Ti based etch by product redeposition. When higher source power (800 W) is used, the trench profile is tapered due to a pronounced hard mask faceting. Higher source power leads to higher plasma dissociation and ion bombardment conditions, which explains the hard mask faceting. This trend is in good agreement with the results presented in a previous work describing the hard mask faceting mechanisms [4]. The patterning of dense SiOCH with the baseline process leads also to profile distortions attributed to TiF_x species, even if this process does not lead to profile distortions with the porous SiOCH.

All of those results show that the main critical dimension issues for the patterning of narrow p-SiOCH trenches are:

(1) Profile distortion due to Ti-based etch by-product redeposition on the trench sidewalls which is observed at low chuck temperature (20 °C), at low pressure (50 mTorr), with polymerizing etching chemistry (CH_2F_2 addition to the CF_4/Ar gas mixture) and when dense SiOCH is etched with the baseline process.

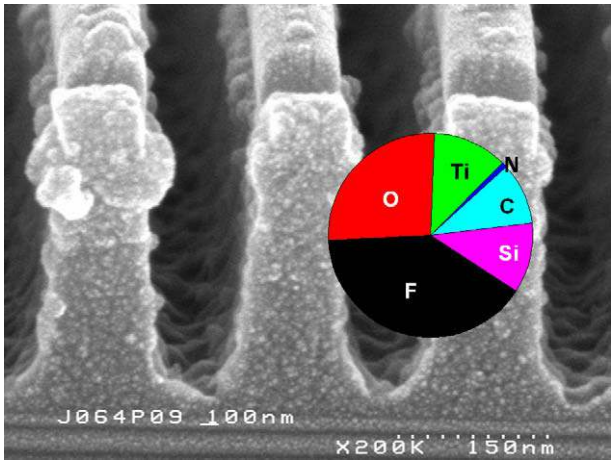

Fig. 10. Porous SiOCH trenches etched with the process at 20 °C and chemical composition of the sidewalls determined by XPS.

(2) Tapered profile due to hard mask faceting at high source power (600 W of source power).

With the baseline process, we can pattern p-SiOCH trenches down to 60 nm width. It has to be noticed that undulation of the dielectric lines is observed for trench dimensions lower than 100 nm when TiN is used as a hard mask (Fig. 12). This phenomenon is discussed in details elsewhere [26].

3.2.3. Mechanisms of Ti-based etch by-product redeposition

The results presented in the previous section highlight that Ti-based deposits are responsible for the profile distortion of p-SiOCH trenches. The TiF_x deposits originate from the etching or sputtering of the top surface of the fluorinated TiN hard mask generated during the exposure to the fluorocarbon plasma etch process. Temperature is one of the key parameters that prevent the TiF_x-based deposits since an increase of the wafer temperature up to 60 °C strongly minimizes the formation of TiF_x deposits on the trench sidewalls. It has to be noticed that slight modifications of the baseline process lead to severe profile distortions, indicating that the process window is very narrow. Indeed, our experiments show that a decrease in the wafer temperature and pressure or the addition of a polymerizing gas in the etching chemistry favor the formation of TiF_x deposits on the trench sidewalls.

Previous studies on the etching of TiN in fluorocarbon-based plasmas have shown that TiN etching is mainly driven by an ion-assisted chemical etching mechanism, and that the etch rate is controlled by the fluorine concentration in the plasma gas phase, the wafer temperature, and the ion bombardment density and energy [4]. In fluorocarbon-based plasmas, the TiN top surface is highly fluorinated with a small amount of carbon and the etch by-products in the gas phase are mainly TiF_x and CNF_x [4]. Fracassi and d'Agostino have also reported the presence of TiF_3 and TiF_4 species on the TiN surface after exposure to CF_4/O_2 plasmas. They have shown that the bottleneck for TiN etching is the last step of fluorination in which the volatile TiF_4 molecule is produced from TiF_3 [27]. They also reported that the probability of finding TiF_4 adsorbed on the etched surface is dramatically reduced by increasing the temperature [27].

Based on the knowledge on TiN etching in fluorocarbon plasmas, we can propose the following mechanism explaining the formation of TiF_x deposits on the trench sidewalls. During the etching of p-SiOCH trenches, the surface of the TiN hard mask is fluorinated (TiF_x like surface with a small amount of carbon). The fluorinated TiN surface results from the synergy between the fluorine reactive species and the ion bombardment, leading to the formation of TiF_x etch by-products in the plasma. Depending on the volatility of TiF_x species, they are either pumped out of the plasma chamber or redeposited on any surface exposed to the plasma (chamber walls and wafer [11]). The volatility of TiF_x compounds depends on the wafer temperature and on the number of fluorine atoms into the TiF_x molecule. A variation in fluorine concentration or in the ion energy flux (ion energy x ion density) can significantly change the composition of TiF_x etch products present in the gas phase and consequently their volatility. It has to be noticed that TiF_x species can also be dissociated or recombined with reactive species (such as fluorine atoms) in the plasma. Those reactions contribute to the balance between volatile species (such as TiF_4) and non volatile species concentrations into the plasma gas phase.

Experimentally, we have shown the presence of TiF_x deposits on the trench sidewalls at a substrate temperature of 20 °C in a CF_4 / Ar plasma, while no deposit is clearly evidenced on porous SiOCH patterned structures at 60 °C. This indicates that the deposition of Ti-based compounds can be minimized at higher substrate temperature by increasing their volatility. We have also observed that TiF_x species get deposited on the trench sidewalls with the addition of

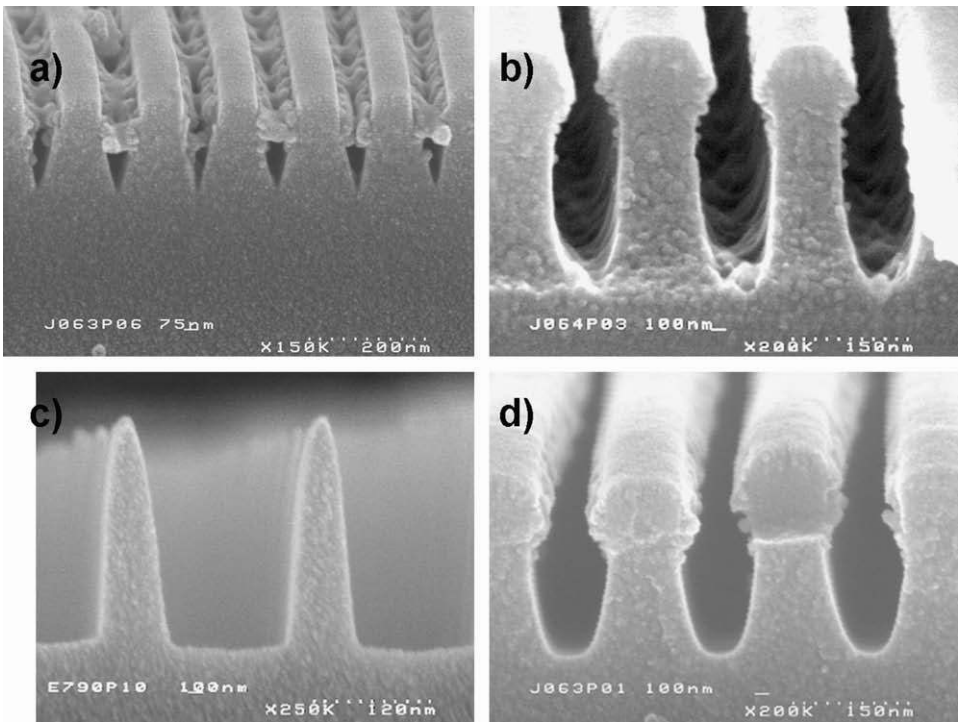

Fig. 11. Porous SiOCH trenches etched with different plasma parameters (a) lower pressure (50 mTorr), (b) 7 sccm CH_2F_2 addition, (c) higher source power (600 W), (d) dense SiOCH trenches.

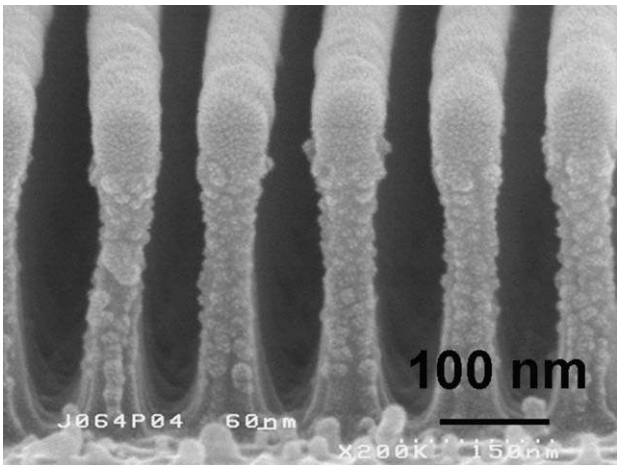

Fig. 12. 60 nm width porous SiOCH trenches etched with a TiN hard mask Wiggling is not observed thanks to a specific design.

CH_2F_2 in a CF_4/Ar plasma or when dense SiOCH is etched at a substrate temperature of 60 °C. This indicates a lower volatility of the TiF_x compounds which can be attributed to a change in the composition of the TiN etch by-products present in the plasma gas phase. In both conditions, pressure and power are kept constant, so that we can assume that the ion flux, the ion energy and the electron temperature are similar. The change in the TiF_x species composition can be explained by a variation of the fluorine concentration in the gas phase. When the plasma is fed with CH_2F_2 instead of CF_4, the fluorine concentration in the plasma is expected to decrease. Indeed there are only two fluorine atoms per CH_2F_2 molecule instead of four fluorine atoms per CF_4 molecule. Furthermore, hydrogen is known to scavenge fluorine, which also contributes to decreasing the fluorine concentration in the plasma [28]. In our experimental conditions, we cannot estimate accurately the fluorine concentration by actinometry. However, a previous study has clearly pointed out the decrease in fluorine concentration in the gas phase of a CF_4 inductively coupled plasma when CH_2F_2 is added instead of CF_4 [4]. In our work, the profile distortions observed with CH_2F_2 addition in the etching chemistry can then be attributed to the decrease in fluorine concentration in the plasma leading to a lower volatility of the TiF_x compounds. It can also explain the presence of residues when the pressure (and thus the concentration of fluorine) is decreased. When dense SiOCH dielectric structures are etched in a CF_4 / Ar plasma, the etching of the material increases the loading of the fluorine atoms, generating a decrease of the concentration of fluorine in the plasma. To confirm this assumption, we have performed the etching of TiN masked silicon trenches in order to change the fluorine concentration by increasing even more the loading of fluorine radicals. Indeed the fluorine concentration in the plasma is directly impacted by the material being etched: an increase in silicon in the material will consume more fluorine by forming volatile SiF_2 and SiF_4 molecules. Therefore, in our experiments more fluorine will be loaded in CF_4 / Ar plasmas when going from p-SiOCH to dense SiOCH and finally to pure silicon. As a consequence, the formation of poorly volatile TiF_x products will increase when going from p-SiOCH to dense SiOCH and finally to bare silicon. In these experimental conditions, all the plasma parameters are kept constant (pressure, power, gas feed,...). Thus, in that case, we can consider that the change in the concentration of free fluorine in the plasma is mainly attributed to the difference in loading of fluorine by the etching of the materials. By estimating the consumption rate of fluorine by the etching of the different materials, we have then a direct approximation of the variation of the fluorine concentration in the plasma. We have estimated the fluorine loading during the etching of the different materials (porous SiOCH, dense SiOCH and Si). Since silicon etch by-products are mainly SiF_2 and SiF_4, we can roughly estimate that the consumption of one silicon atom leads to the loading

of three fluorine atoms and that each hydrogen atom in the etched material loads one fluorine atom from the plasma. Taking into consideration the amount of material etched (based on the material density, the etched thickness and the open area on the wafer) and the composition of the material, we can estimate the flux of fluorine d_F consumed during the etching by

$$d_F = \frac{\rho * S * \tau * d}{\tau * 1.66 \times 10^{-24} * V * \sum_i \%_i * m_i}(3 * \%_{Si} + \%_h),$$

where d_F is the loading rate of fluorine (in $cm^{-3}\ s^{-1}$), ρ the material density (in g cm^{-3}), S the wafer surface (in cm^2), τ the open area ratio of the mask, (estimated to 0.8), d the etched depth (in cm), t the etching time (in s) and V the volume of the reactor (in cm^3). $\%_i$ and m_i are the atomic proportion and the mass (in amu) of element i (Si, H, C or O), respectively. The material composition is given by the material supplier or estimated by XPS (considering three hydrogen atoms per carbon atom). The material density is estimated by XRR. (Table 1). The loading rate of fluorine (d_F) corresponds to the number of free fluorine atoms consumed by the etching of the material per second and per cubic centimeter. To facilitate the understanding, this loading rate can be expressed in sccm as shown in Table 1. During the etching of Si trenches, a fluorine loading of 56 sccm is estimated whereas a much lower fluorine loading is observed during the etching of porous SiOCH (10 sccm) or dense SiOCH (14 sccm). The higher loading of fluorine radicals during the etching of Si leads to a much lower fluorine concentration in the plasma. The SEM pictures (Fig. 13) indicate a strong profile distortion of the Si trenches due to a huge Ti-based deposit on the sidewalls while no profile distortion of the porous SiOCH trenches is evidenced. It has to be noticed that the process was not optimized to etch silicon, and that a fluorocarbon layer is probably formed on trenches sidewalls and contribute to the profile distortion. However, the non-conformity of the coating on the sidewalls indicates that profile distortion is mainly attributed to TiF_x species. This difference in terms of trench profile is well correlated to the amount of fluorine in the plasma: a decrease in fluorine concentration in the plasma gas phase during silicon etching favors the formation of Ti-based deposit on the trench sidewalls (strong profile distortion of silicon trenches). This behavior is also confirmed by the etching of dense SiOCH trenches. The calculated fluorine flow loaded during the dense SiOCH etching (14 sccm) is slightly higher than the flow of fluorine consumed during the etching of p-SiOCH. As a consequence, less free fluorine is available in the plasma, and more non volatile TiF_x species are formed during the etching of dense SiOCH, leading to the slight profile distortion depicted in Fig. 11, while no profile distortion is observed during p-SiOCH etching (Fig. 9). The whole results indicate that to prevent the deposition of TiF_x species, the plasma must be rich in fluorine and the substrate temperature must be at least 60 °C, which corresponds to conditions favoring the etching of TiN.

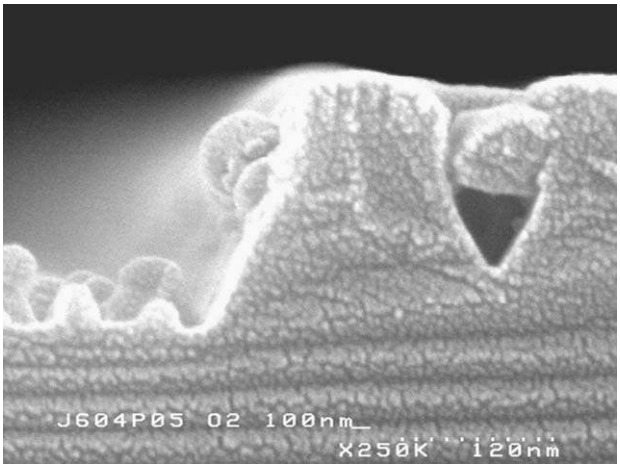

Fig. 13. Silicon trenches etched with a TiN hard mask using the baseline etch process.

4. Conclusion

In this paper, we have investigated the etching of porous SiOCH trenches etched with a TiN hard mask. Such a hard mask presents a slight oxidized top surface which must be removed by a chlorine containing breakthrough plasma step. Thus, narrow trenches (down to 40 nm width) can be opened into TiN with a slight CD bias (around 10 nm) attributed to $C_xH_yCl_z$ and SiO_xCl_y deposits on the photoresist and TiN sidewalls during the etching.

Using TiN instead of SiO_2 as a hard mask leads to severe profile distortions, attributed to poorly volatile TiF_x etch by-products which get deposited on the trench sidewalls. Such TiF_x species originate from the etching or sputtering of the fluorine-rich TiN surface during the fluorocarbon-based plasma exposure. A high chuck temperature (60 °C) and fluorine-rich plasma conditions are required to limit TiF_x species redeposition by increasing their volatility. The etch process window is narrow to achieve sub-100 nm width trenches. After optimization of the etch process (CF_4 / Ar-based plasma), we can pattern porous SiOCH trenches down to 60 nm width. However, dielectric lines undulations (wiggling phenomenon) are observed for trench widths lower than 100 nm.

Acknowledgement

We acknowledge the support of the European Commission to the project PULLNANO under contract No IST-026828 from the Information Society Technologies Program (IST) within the European Union's Sixth RTD Framework Program.

References

[1] K. Maex, M.R. Baklanov, D. Shamiryan, F. Iacopi, S.H. Brongersma, Z.S. Yanovitskaya, J. Appl. Phys. 93 (2003) 8793.
[2] O. Hinsinger, R. Fox, E. Sabouret, C. Goldberg, C. Verove, W. Besling, P. Brun, E. Josse, C. Monget, O. Belmont, J. Van Hassel, B.G. Sharma, J.P. Jacquemin, P. Vannier, A. Humbert, D. Brunel, R. Gonella, E. Mastromatteo, D. Rebert, A. Farcy, J. Muel Demonstration of an extandable and industrial 300mm BEOL integration for the 65-nm technology node; Int. Electron. Devices Meeting (2004).
[3] N. Posseme, T. David, M. Darnon, T. Chevolleau, O. Joubert, Int. Conf. Microelectron. Interfaces (2005).
[4] M. Darnon, T. Chevolleau, D. Eon, L. Vallier, J. Torres, O. Joubert, J. Vac. Sci. Technol. B 24 (2006) 2262.
[5] F. Iacopi, Y. Travali, B. Eyckens, C. Waldfried, T. Abell, E.P. Guyer, D.M. Gage, R.H. Daskardt, T. Sajavaara, K. Houthoofd, P. Grobet, P. Jacobs, K. Maex, J. Appl. Phys. 99 (5) (2006) 053511.
[6] Ch. Le Cornec, F. Ciaramella, V. Jousseaume, P. Leduc, A. Zenasni, G. Passemard, Microelectron. Eng. 83 (11–12) (2006) 2122–2125.
[7] N. Posseme, T. Chevolleau, O. Joubert, L. Vallier, P. Mangiagalli, J. Vac. Sci. Technol. B 21 (2003) 2432.
[8] F.H. Bell, O. Joubert, L. Vallier, J. Vac. Sci. Technol. B 14 (1) (1996) 96.
[9] M. Armacost, P.D. Hoh, R. Wise, W. Yan, J.J. Brown, J.H. Keller, G.A. Kaplita, S.D. Halle, K.P. Muller, M.D. Naeem, S. Srinivasan, H.Y. Ng, M. Gutsche, A. Gutmann, B. Spuler, IBM J. Res. Dev. 43 (1999) 39.
[10] S. Ma, M. Jain, J.D. Chinn, J. Vac. Sci. Technol. A 16 (3) (1998) 1440.
[11] T. Chevolleau, M. Darnon, T. David, N. Posseme, J. Torres, O. Joubert, J. Vac. Sci. Technol. B 25 (2007) 886.
[12] J.H. Scofield, J. Electron. Spectroscop. Relat. Phenom. 8 (1976) 129.
[13] F. Fracassi, R. d'Agostino, R. Lamendola, I. Mangieri, J. Vac. Sci. Technol. A 13 (1995) 335.
[14] P. Prieto, R.E. Kirby, J. Vac. Sci. Tehnol. A 13 (1995) 2819.
[15] J. Halbritter, H. Leiste, H.-J. Mathes, P. Walk, H. Winter, Solid State Commun. 68 (12) (1988) 1061–1064.
[16] E. Pargon, O. Joubert, S. Xu, T. Lill, J. Vac. Sci. Technol. B 22 (2004) 1869.
[17] T.J. Dalton, J.C. Arnold, H.H. Sawin, S. Swan, D. Corliss, J. Electrochem. Soc. 140 (8) (1993) 2395–2401.

[18] A. Le Gouil, O. Joubert, G. Cunge, T. Chevolleau, L. Vallier, B. Chenevier, I. Matko, J. Vac. Sci. Technol. B 25 (3) (2007) 767–778.
[19] L. Desvoivres, L. Vallier, O. Joubert, J. Vac, Sci. Technol. B 19 (2) (2001) 420–426.
[20] M. Kogelschatz, G. Cunge, N. Sadeghi, J. Vac, Sci. Technol. A 22 (3) (2004) 624–635.
[21] X. Detter, R. Palla, I. Thomas-Boutherin, E. Pargon, G. Cunge, O. Joubert, L. Vallier, J. Vac. Sci. Technol. B 21 (5) (2003) 2174–2183.
[22] E. Pargon, O. Joubert, T. Chevolleau, G. Cunge, S. Xu, T. Lill, J. Vac. Sci. Technol. B 23 (1) (2005) 103–112.
[23] I. Tepermeister, N. Blayo, F.P. Klemens, D.E. Ibbotson, R.A. Gottscho, J.T.C. Lee, H.H. Sawin, J. Vac. Sci. Technol. B 12 (1994) 2310.
[24] G.S. Oehrlein, Surf. Sci. 386 (1997) 222–230.
[25] Y. Furukawa, M. Patz, T. Kokubo, J.H.M. Snijders, Microelecron. Eng. 70 (2003) 267.
[26] M. Darnon, T. Chevolleau, O. Joubert, S. Maitrejean, J.C. Barbe, J. Torres, Appl. Phys. Lett. 91 (2007) 194103.
[27] F. Fracassi, R. d'Agostino, Pure and Appl. Chem. 64 (5) (1992) 703–707.
[28] R.A.H. Heinecke, Solid State Electron. 18 (1975) 1146–1147.